COMPARATIVE ANALYSIS OF LAND COVER MAPPING TECHNIQUES ON A MEDITERRANEAN LANDSCAPE USING FORMOSAT-2

Montasser Jarraya[1], Ioannis Manakos[1,2], Chariton Kalaitzidis[1], and George Vozikis[3]

1. Department of Geoinformation in Environmental Management, Mediterranean Agronomic Institute of Chania (MAICh) Alsyllio Agrokepiou, 73100, Greece; E-mail: Chariton(at)maich.gr
2. Information Technologies Institute, Centre for Research and Technology Hellas (CERTH), Building A, 6km Harilaou-Thermi, PO Box 60361, Thessaloniki, 57001, Greece, E-mail: imanakos(at)iti.gr
3. Spot Infoterra Hellas SA, GEO-Information Services ASTRIUM SERVICES, Ipirou street & Etolias Chalandri, 15 231, Greece; E-mail:george.vozikis(at)spotinfoterra.gr

ABSTRACT

Landscape fragmentation is quite dominant in Mediterranean regions and poses significant problems in semi-automatic satellite image classification methods. The issue is somewhat alleviated when high spatial resolution data are used, allowing the production of detailed classification schemes, using either pixel- or object-based classification methods.

The main objective of this research is the comparison of classification methods for Land Use/Land Cover (LU/LC) mapping using high spatial resolution data provided by the FORMOSAT-2 satellite. Three pixel-based and an object-based classification approaches are evaluated; the pixel-based methods employing the Support Vector Machine (SVM), Maximum Likelihood (ML), and Artificial Neural Network (ANN) algorithms, and the object-based classification using the Nearest Neighbour classifier.

All three methods were assessed and compared to each other with respect to the overall and individual accuracy of their classification results, in order to determine the most efficient method. The comparison was made both in terms of overall classification accuracy as well as in terms of individual class identification accuracy. The differences in the performance of each classification method are discussed.

INTRODUCTION

Landscape fragmentation is a threat to sustainable ecosystem management in the Mediterranean region (1). It represents the alteration in the composition and spatial arrangement of landscape elements, consequently affecting population and ecosystem processes (2,3). The classification of remotely sensed images is an important asset for the determination of Land Use and/or Land Cover (LU/LC) information (4,5).

Among the most popular and widely used classification algorithms is the Maximum Likelihood (ML) classifier (6,7,8,9,10,11,12,13,14,15). Limitations while using the ML classifier lie in the difficulty of integrating spectral data with ancillary data as well as in the fact that unbalanced distribution of training samples could introduce errors to the image classification procedure (11). To overcome such issues, non-parametric classification techniques such as Artificial Neural Network (ANN), Support Vector Machine (SVM), and Nearest Neighbour (NN) within an Object Based classification approach have been introduced recently (9,16,17,18,19).

ANN has emerged as an important tool for classification. Its success is based on the utilisation of non-linear models, which make neural networks flexible in modelling real-world multifaceted relationships (20). Detailed descriptions of the definitions of the ANN parameters with reference to their concepts, algorithms, as well as their potentials and limitations are mentioned in (21,22,23,24).

SVM has proved to be a theoretical superior machine learning methodology (25) with interesting results in pattern recognition, particularly for supervised classification of high-dimensional data sets (9,10,13,17,18,25,26,27,28,29). SVM functions by non-linearly projecting the training data to a feature space of higher dimensions, using a kernel function. This results in a data set separable by a linear classifier. This process enables the classification of remote sensing data sets, which are usually not linearly separable. Classification in high-dimension feature spaces often results in over-fitting of the data, while at the same time it is controlled through the principle of structural risk minimization in SVM (30). More comprehensive descriptions of the operation of the method may be found in (25,31,32).

In contrast to pixel-based classification methods, object-based classification first aggregates image pixels into spectrally homogenous image objects via an image segmentation algorithm, and then classifies the resulting individual objects (33). In fact, the main advantage of Object Based Image Analysis (OBIA) is the combination of the spectral information with spatial and topological characteristics (33). Literature contains numerous studies that demonstrate both the advantages and the limitations of the approach (34,35,36,37,38,39,40,41,42,43).

A comparison of the four classification methods for LU/LC mapping using FORMOSAT-2 imagery was performed, providing results that can support decision making and optimize users' feedback. The classification performance of each method is subsequently discussed.

METHODS

Test site

The study area is the Akrotiri peninsula in North-West Crete, Greece (Figure 1). It lies at the centre of a broad low-slope plateau at 35°30′0″ N latitude and 24°04′00″ E longitude. The study area has a widely patchy landscape with a mean altitude of approximately 750 m above sea level. The climate is typically Mediterranean, characterized by a mean monthly temperature varying from 22.8°C to 13.9°C, and a mean monthly precipitation ranging between 11.4 and 93.5 mm during the summer and winter seasons, respectively. The land cover in the study area is highly fragmented and principally used for agriculture and other anthropogenic activities, such as small-scale industry, while the areas of natural vegetation consist mainly of phrygana, dominated by shrublands (44).
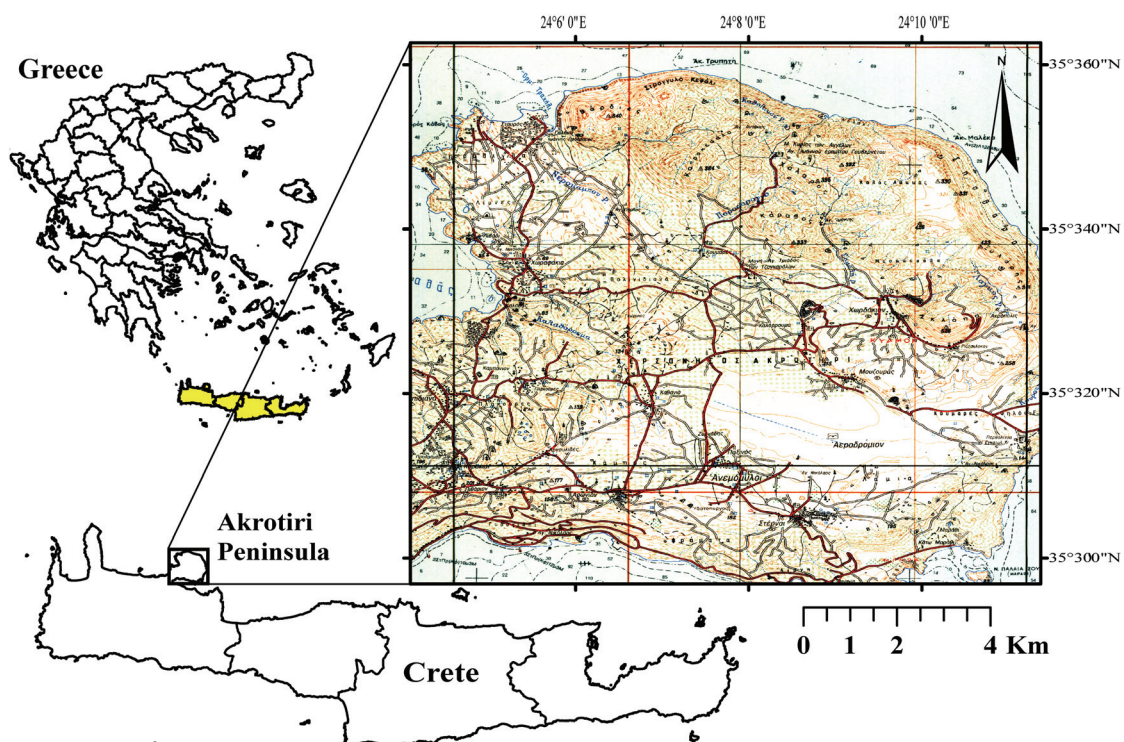

Figure 1: The study area location.

The LU/LC types of the study area

The Mediterranean LU/LC types may be reflected in the nomenclature of the Corine Land Cover (2006) (CLC 2006) according to the following table:

Table 1: Corine Land Cover (2006) Levels and the associated classes.

CLC_C	LEVEL1	Abr*	LEVEL2	Abr	**LEVEL3**	Abr
111	Artificial surfaces	AS	Urban fabric	UF	**Continuous urban fabric**	CUF
112	Artificial surfaces	AS	Urban fabric	UF	**Discontinuous urban fabric**	DUF
123	Artificial surfaces	AS	Industrial, commercial and transport units	ICTU	**Port areas**	PA
124	Artificial surfaces	AS	Industrial, commercial and transport units	ICTU	**Airports**	A
131	Artificial surfaces	AS	Mine, dump and construction sites	MDCS	**Mineral extraction sites**	MES
141	Artificial surfaces	AS	Artificial, non-agricultural vegetated areas	ANAVA	**Green urban areas**	GUA
211	Agricultural areas	Aareas	Arable land	AL	**Arable land**	AL
241	Agricultural areas	Aareas	Heterogeneous agricultural areas	HAA	**HAA**	HAA
223	Agricultural areas	Aareas	Permanent crops	PC	**Olive groves**	OG
231	Agricultural areas	Aareas	Pastures	P	**Pastures**	P
323	Forest and semi natural areas	FSNA	Scrub and/or herbaceous vegetation associations	SHVA	**Sclerophyllous vegetation**	SV
321	Forest and semi natural areas	FSNA	Scrub and/or herbaceous vegetation associations	SHVA	**Natural grasslands**	NG
331	Forest and semi natural areas	FSNA	Open spaces with little or no vegetation	OS	**Beaches, dunes, sands**	BDS
332	Forest and semi natural areas	FSNA	Open spaces with little or no vegetation	OS	**Bare rocks**	BR
333	Forest and semi natural areas	FSNA	Open spaces with little or no vegetation	OS	**Sparsely vegetated areas**	SVA
523	Water bodies	WB	Marine waters	MW	**Sea and ocean**	SO

* Abr stands for "Abbreviation" and CLC_C stands for "Corine Land Cover Code".

The third level of CLC (2006) is considered to be descriptive enough for the study area. The classification scheme used herein included sixteen classes, written in bold letters in the table above.

Available data

FORMOSAT-2 is a Taiwanese satellite, operational since May 2004 on a sun-synchronous orbit, with an on-board Remote Sensing Instrument (RSI). RSI provides high spatial resolution images (a) of 8 m in the multispectral mode, in four narrow spectral bands ranging from 0.45 μm to 0.90 μm (blue (B), green (G), red (R) and near-infrared (NIR)), and (b) of 2 m in panchromatic mode (45). The multispectral bands of FORMOSAT-2 imagery (25 Apr 2009) were used, since it pre-

sents a good compromise between high spatial and temporal resolution, and relative low acquisition budget (10). The image was georeferenced to the Geographic Lat/Lon projection system under the Datum WGS-84 using ENVI software package version 4.7. In addition, the image was radiometrically calibrated to the top of the atmosphere radiance and subsequently atmospherically corrected using the FLAASH module in ENVI software.

In order to estimate the Leaf Area Index (LAI), first, the Normalized Difference Vegetation Index (*NDVI*) was calculated from the FORMOSAT-2 image following Eq. (1):

$$NDVI = \frac{NIR - R}{NIR + R}$$

(1)

Using the results of (46), *LAI* was computed by Eq. (2):

$$LAI = -1.323 \ln \frac{0.88 - NDVI}{0.714}$$

(2)

The authors (46) used this equation, which links *NDVI* with *LAI* using *in situ NDVI* measurements that show a very good fitness between *NDVI* and *LAI* according to a negative exponential function ($r^2 = 0.987$). Their work was applied in an evergreen scrub oak ecosystem in Florida. However, due to the differences between the evergreen scrub oak and the tested ecosystem in the current study, a hypothesis is made about the suitability of the second equation for the latter.

Training and validation data

For the collection of the training sites (Table 2), random sampling was performed within the study area, selecting numerous samples to ensure that all classes were adequately represented (47,48). According to (49) and (50) a minimum of $10P$ to $30P$ pixels per class should be used for the training set, where P is the number of bands used. For instance, in the current study, random selection was made through FORMOSAT-2 image with a mean of 299 pixels per class. The selection of the training sets was based on the spectrally purest pixels per class, based on visual on-screen inspection.

Validation points were generated through stratified random sampling on the thematic product map produced by SVM using the linear kernel on image composition B (see next chapter). Multinomial distribution was chosen in this study to determine the number of validation sites required, since it provided the adequate sample size for generating an error matrix (48). The following Eq. (3) was used to determine the necessary sample size:

$$n = \frac{B(1 - \Pi_i)}{b_i^2 \Pi_i}$$

(3)

Where *n* is the sample size generated, Π_i ($i = 1, ..., k$) is the proportion in category *i*, b_i represents the absolute precision of the sample and *B* is determined from a Chi-square table with one degree of freedom and $1 - a/k$. The result of the equation was a mean of 65 points per class, and hence, a total of 1,046 points were generated, sufficient for statistically significant results (48). A total of 57 points were selectively referenced in the field. The remaining validation points were identified using the panchromatic band of FORMOSAT-2 in combination with Google Earth's high resolution image for the area, dated 13 Aug 2009 (Table 2).

The spectral separability of the training and validation data sets was examined by a Jefferies-Matusita and transformed divergence separability tests (51). The spectral separability of a selected point was calculated for each set in reference to a number of spectral channels of the input image. The Region Of Interest (ROI) separability analysis demonstrated that some classes (artificial surface classes, natural grassland and heterogeneous agricultural areas, olive groves and sclerophyllous vegetation) have a low separability index (less than 1), but when the *NDVI* and subsequently *LAI* were incorporated as additional input bands, the separability index increased.

Sea and Ocean class accounted for more than 84% of the surface of the image with uniform spectral distribution. Therefore it was masked out and excluded from the accuracy assessment procedure.

Overall accuracy expresses a quantification of the overall accuracy of classification and is expressed in terms of percentage. The kappa coefficient (K) expresses the proportionate reduction in error generated by a classification process, compared with the error of a completely random classification (52,53).

Table 2: Validation and distribution of training points among classes.

classes	Validation points		Training points
	Identified via image analysis	Via points from the field	
AL	62	2	462
BDS	9	0	61
BR	82	0	658
CUF	114	0	920
DUF	20	0	77
GUA	8	5	75
HAA	83	0	191
MES	20	0	85
NG	46	10	333
OG	69	13	457
P	5	0	15
PA	5	0	75
SH-SVA	6	0	164
SO	0	0	219
SV	150	21	684
SVA	290	6	395
airport	20	0	170
Total	989	57	
Final Total	1046		5041

Classification procedure

Two approaches were tested in the current study, the pixel-based and the object-based classifications. For the pixel-based approach the Support Vector Machine (SVM), Artificial Neural Network (ANN) and the Maximum Likelihood (ML) algorithms were employed, and for the object-based classification the Nearest Neighbour (NN) algorithm was used.

Initially, four bands were used in the classification scheme of the FORMOSAT-2 image (Blue, Green, Red, and Near infrared) (image composition A). A second image composition was subsequently generated by stacking the *NDVI* layer with the four original spectral bands of FORMOSAT-2 image (image composition B). A third image composition was created by combining both *LAI* and *NDVI* layers with the four spectral bands of FORMOSAT-2 image (image composition C). This was decided in order to gain an insight into the sensitivity of the overall ML and SVM results to the band combination used as input in their parameterization stages. Secondly, it would allow us to identify the band combination to be used for the final comparison between the four classifiers chosen in this study, SVM, ANN, ML, or OBIA (NN).

ML allocates a pixel to the class with the highest probability of membership (54). Unlike ML, ANN provides an alternative to traditional statistical classification approach, as it is more flexible and may map nonlinearity among variables without assumptions about the data (55). Multi-layered feed-forward ANN was applied by a logistic activation function, which was implemented to classify the FORMOSAT-2 imagery. ANN was introduced using a training threshold contribution value of 0.9, a training rate of 0.2, a training momentum of 0.9 and a training root-mean-square error (*RMSE*) exit criteria of 0.1. The number of training iterations was set to 1,000, and one hidden layer was used.

SVM has been developed on a solid base of statistical learning theory (30), and it is considered to be an original learning algorithm for neural networks, which absolutely avoids the problem of layer number selection and hidden unit numbers (9). In the present study, a multiclass SVM pair-wise classification strategy was applied. A number of studies have indicated that the kernel selection is important for the performance of the SVM classifier (10,13,56). Three kernel functions were used in the present study:

Linear function: $$k\left(x_i, x_j\right) = x_i^T x_j \tag{4}$$

Polynomal function: $$k\left(x_i, x_j\right) = \left(y x_i^T x_j + r\right); \ \gamma > 0 \tag{5}$$

Radial basis function (*RBF*): $$k\left(x_i, x_j\right) = \exp\left(-\gamma \left\|x_i, x_j\right\|^2\right); \ \gamma > 0 \tag{6}$$

where parameter γ exists in all kernels except for the linear kernel, *d* is the polynomial degree, and *r* is the bias term in the polynomial kernel. Parameters γ, *d* and *r* are defined by the user following the trial and error iteration procedure, as their correct definition significantly increases the accuracy of the SVM solution. In this study, parameterizations were based on results of previous studies (10,13,26) as well as on trial and errors tests which are not presented here.

OBIA presents a methodological framework for machine-based interpretation of complex classes, defined by spectral, spatial, and structural, as well as hierarchical properties (57,58). In the current paper, the classification was performed using the eCognition software package (version 7) with the standard Nearest Neighbour classifier. The training objects were selected using the overlay rule of the randomly distributed pixels as described in the section *Training and validation data*. A hierarchical classification strategy was followed using initially the first level of CLC (2006) in order to break down the image on four major classes, namely agriculture areas, water body (WB), artificial surface, forest and seminatural areas, including the class of shadowed sparsely vegetated areas (SH-SVA). Then a more detailed segmentation and classification were performed for each class of the first level except WB and SH-SVA, which remain the same across all CLC (2006) levels.

The multiresolution segmentation of the first level was performed with a small-scale factor of 45 and shape and compactness values of 0.1 and 0.9, respectively, followed by a factor of 31 and shape and compactness values of 0.2 and 0.8 for the second level. All the spectral bands of FORMOSAT-2 image were used in this process adding the *NDVI* and *LAI* layers. The band ratios "band Red / band Near Infra Red", "band Green / band Red", and "band Red / band Green" were used complementarily to discriminate the CLC (2006) third level classes.

RESULTS

The results are presented as follows:

a) Selection of the best performing kernel for SVM classifier in comparison with the most popular and widely used ML classifier using image composition A and the three levels of CLC (2006) class categories;

b) Image composition selection by the application of ML and the best performing kernel from (a) on all CLC (2006) levels;

c) Comparison among the four classifiers, namely ML, ANN, SVM, and OBIA (NN) using the resulting selection of the image composition and the best performing kernel to be implemented in the SVM classifier.

Kernel selection

Overall classification of FORMOSAT-2 image composition A using either the ML or the SVM classifier with the three different kernels proved to be quite accurate, but slightly different (for results see Table 3). The three levels of CLC (2006) class categories were used in this process. In the CLC (2006) first level, the three kernels produced the same results with 77% and 0.5493 for the overall accuracy assessment and *K*, respectively, whereas 73.83% and 0.577 were registered for ML. In the CLC (2006) second level, kernels demonstrated somewhat different results with the polynomial kernel reaching 75.72% and 0.6877 for overall accuracy assessment and *K*, respectively, and the

lowest results were registered by ML with 59.2% and 0.5111. The CLC (2006) third level, which was used in later steps, showed best performance of the *RBF* kernel against the other kernels and ML classifier with 79.2% and 0.7564 as overall accuracy assessment and *K*, respectively. Only 62.35% and 0.5718 were achieved by ML. That could be explained by the fact that SVM defines decision boundaries between classes using support vectors instead of statistical attributes, which depend on the number of training sites used.

Table 3: Overall accuracy assessment results and Kappa coefficient for ML and SVM classifiers for the three levels of CLC (2006) using image composition A (B, G, R, and NIR).

CLC (2006)_level 1				
	ML	SVM-Linear_K*	SVM-Polynomial_K	SVM-RBF_K
Overall Accuracy	73.83%	77.00%	77.00%	77.00%
Kappa Coefficient	0.5777	0.5493	0.5493	0.5493
CLC (2006)_level 2				
	ML	SVM-Linear_K	SVM-Polynomial_K	SVM-RBF_K
Overall Accuracy	59.20%	69.85%	75.72%	74.62%
Kappa Coefficient	0.5111	0.6043	0.6877	0.6709
CLC (2006)_level 3				
	ML	SVM-Linear_K	SVM-Polynomial_K	SVM-RBF_K
Overall Accuracy	62.35%	77.67%	76.43%	79.20%
Kappa Coefficient	0.5718	0.7378	0.7246	0.7564

* *K* stands for kernel type

According to the results analysed in Table 3, the *RBF* kernel demonstrated the best performance in the third level of CLC (2006), while the polynomial kernel performed better in the second level. Since the CLC (2006) third level is considered to be descriptive enough for the study area, the *RB*F kernel is selected for further analysis.

Image composition selection

SVM produced higher classification accuracy in comparison to ML in all the three levels of CLC (2006) with significant results in terms of overall accuracy and kappa coefficient, especially for the second and third levels (Table 4).

Table 4: Overall accuracy assessment results and Kappa coefficient for ML and SVM classifier for the three image compositions (A, B and C).

CLC (2006)_level 1						
	ML(A)*	ML(B)*	ML(C)*	SVM(A)	SVM(B)	SVM(C)
Overall Accuracy	73.83%	78.05%	71.28%	77.00%	77.60%	78.07%
Kappa Coefficient	0.5777	0.6342	0.5421	0.5493	0.5547	0.5633
CLC (2006)_level 2						
	ML(A)	ML(B)	ML(C)	SVM(A)	SVM(B)	SVM(C)
Overall Accuracy	59.20%	61.68%	62.12%	74.62%	73.16%	72.56%
Kappa Coefficient	0.5111	0.529	0.5333	0.6709	0.6508	0.6405
CLC (2006)_level 3						
	ML(A)	ML(B)	ML(C)	SVM(A)	SVM(B)	SVM(C)
Overall Accuracy	62.35%	66.54%	64.82%	79.20%	82.94%	87.42%
Kappa Coefficient	0.5718	0.6152	0.5938	0.7564	0.8005	0.8521

*Note: (A), (B), and (C) stand for image composition A, B, and C, respectively

Out of the three levels of CLC (2006) and the three image compositions A, B, and C tested by ML and SVM, image composition C coupled with SVM produced the highest classification accuracy followed by image composition B and then image composition A. Following these results, image composition C, was selected for further analysis.

Classification accuracy comparison for the four classifiers

Table 5 shows the accuracy assessment results for the four classifiers using image composition C with the producer and user accuracies, as well as overall accuracy and kappa coefficient. The classified images are shown in Figure 2. According to the results, SVM showed a better overall performance as compared to OBIA (NN), ANN, and ML classifiers.

Table 5: Accuracy assessment results for the four classifiers using image composition (C).

Abr*	ML		SVM (RBF)		ANN		OBIA (NN)	
Class	Prod.Acc** %	User.Acc %	Prod.Acc %	User.Acc %	Prod.Acc %	User.Acc %	Prod.Acc %	User.Acc %
AL	81.25	77.61	100	94.12	68.75	95.65	100	82.05
BDS	100	47.37	100	75	100	45.45	75	54.55
BR	72.29	59.41	92.77	87.5	95.18	73.15	92.77	88.51
CUF	24.35	52.83	94.78	69.43	94.78	62.29	94.78	68.99
DUF	25	19.23	15	100	0	0	75	88.24
GUA	38.46	55.56	46.15	85.71	0	0	0	0
HAA	39.76	64.71	74.7	86.11	79.52	58.41	95.18	54.48
MES	80	27.12	40	100	40	100	75	88.24
NG	53.57	62.5	87.5	71.01	54.55	51.72	85.71	90.57
OG	80.49	62.26	92.68	90.48	92.68	56.3	98.78	90
P	16.67	7.69	0	0	0	0	100	50
PA	100	15.63	60	100	7	20	60	100
SH-SVA	100	100	100	85.71	100	85.71	83.33	55.56
SV	64.91	85.38	92.98	95.21	44.44	96.2	81.87	66.35
SVA	82.09	81.82	94.93	93.98	81.76	80.67	44.93	96.38
airports	50	31.25	25	100	0	0	80	84.21
Overall Accuracy	64.82%		87.42%		71.07%		76.05%	
Kappa Coefficient	0.5938		0.8521		0.6616		0.7281	
Best performing classifiers	4 out of 16***	1 out of 16	8 out of 16	9 out of 16	4 out of 16	3 out of 16	7 out of 16	5 out of 16

*Abr stands for abbreviation, **Prod Acc and User Acc stand for producer accuracy and user accuracy, respectively. *** "4 out of 16" stands for the example that the ML classifier was more successful in discriminating four classes out of sixteen than the other classifiers were, as shown by the producer accuracy results.

The SVM classifier achieved the highest accuracy among other classifiers by taking into account the good agreement, proved by the *K* value, and the number of classes successfully segregated in both user and producer accuracies. Higher classification accuracies were noticed for agricultural areas than for forest and seminatural areas, and finally for artificial surfaces. However, SVM was not so accurate when classifying classes like pastures, a fact which may be accounted to the inability of the SVM to transform non-linear decision boundaries in a high-dimensional space, in case of low a number of training sites. Another plausible reason for its failure could be the low number of validation pixels. The class of pastures is represented by few sparse patches within the study area.

The same results were noticed with ANN. OBIA (NN) and ML, however, succeeded to demonstrate better classification results in this case.
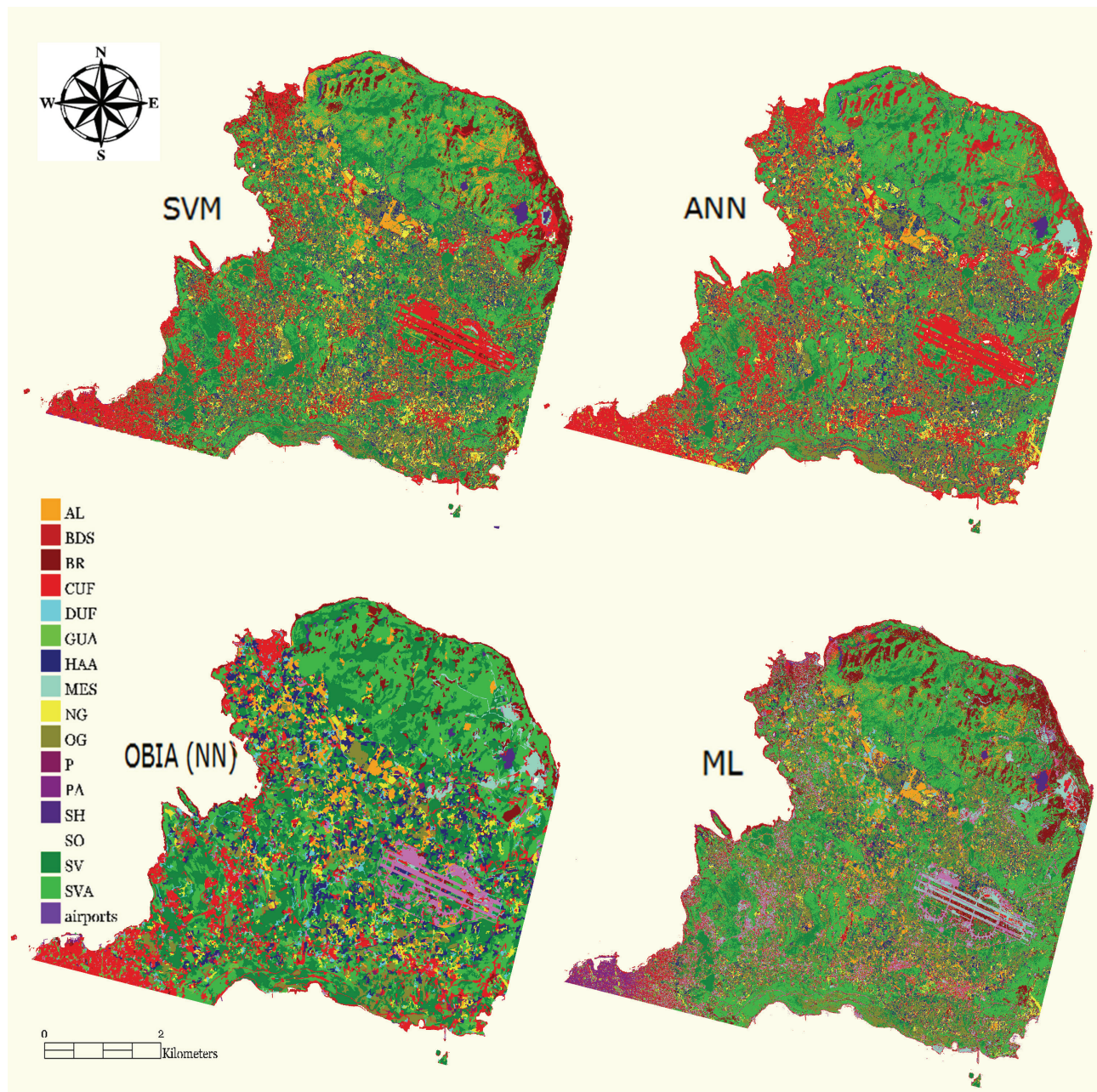

Figure 2: LU/LC classification maps for the four used classifiers, SVM, ML, ANN, and OBIA (NN), respectively.

OBIA (NN) performed better than both classifiers ANN and ML, which is shown in Table 5, with good overall agreement. In addition, it succeeded in discriminating artificial surfaces with the highest overall accuracy. Moreover, sparsely vegetated areas, bare rocks and natural grasslands classes, belonging to the forest and seminatural areas class, were similarly or more successfully discriminated by OBIA (NN) compared to the other classifiers, which shows the potential of the method to gain benefit from the extra added layers, especially *LAI*, in order to set apart the subclasses of forest and seminatural areas (Table 4 and 5). Further processing, not included here for simplicity reasons, supports former statements. However, OBIA (NN) did not accurately classify the green urban areas class, which may be due to the inability of the classifier to separate that class spectrally. The field visit proved that green urban areas and sclerophyllous vegetation classes consist of similar vegetation types, which could be the main reason for their confusion.

Unlike SVM and OBIA (NN), the overall performance of ANN was 71.07% with a good agreement shown by the *K* value of 0.66. Higher producer classification accuracy was noticed among beach dune sands, bare rocks, continuous urban fabric, olive groves, and sparsely vegetated areas classes. On the other hand, ANN performed poorly in classifying discontinuous urban fabric, green urban areas, pastures, and airport classes. The artificial surface classes were confused with each other, especially continuous urban fabric, discontinuous urban fabric, and airports, which may be due to the fact that only one hidden layer was used and also due to the similar spectral signature of the artificial surface classes. Thus, despite the implementation of extra layers in addition to the original four bands of FORMOSAT-2, ANN could not benefit from the spectral information added by those layers.

The ML overall accuracy result was 64.82% with moderate agreement shown by the *K* value of 0.59. Only three classes were discriminated with best success using ML, which are AL, SV, and SVA. In addition, ML produced high rates of commission errors that show the misclassification of similar spectral classes like OG and HAA, as well as artificial surface classes. Furthermore, ML succeeded in distinguishing MES and PA classes, even with small accuracy, within the other classes. Those classes are characterised by small patches, if compared to the whole study area surface. Like ANN, the performance of ML improved by approximately 2% in comparison with the 8% of SVM, which indicates, that the introduction of the extra layers of *LAI* and *NDVI* did not increase the mapping accuracy. This is mostly attributed to the confusion among agriculture areas and artificial surface classes.

For SVM, ANN, and OBIA (NN) classifiers, mineral extraction sites and port areas had extremely low producer accuracies and 100% user accuracies, which indicated that a very small number of pixels were correctly classified as these classes. This could be explained by the small areas representing those classes and by the discriminative potential of those classifiers towards artificial surface classes, especially by OBIA (NN). In addition, it was noticed that the shadowed SVA class was generally classified with 100% accuracy. This indicates that all classifiers tested show a high spectral discrimination capability for this class.

DISCUSSION

In this study, two assumptions were made. The first related to SVM's kernel parameterization, which was based on (10,13 and 32) studies, showing the potential to generate good overall accuracies. The second, related to the *LAI* equation fitness for the study area ecosystem, similarly to the evergreen scrub oak ecosystem presented by (46), which was proved to be of use for the tested ecosystem in the current study.

Among the kernels used in this study, the *RBF* kernel generated the best overall accuracy by performing better than the polynomial and the linear ones. Similar results were produced by (10) using TM data for LU/LC classification testing SVM kernels, *RBF* and Polynomial.

The incorporation of the *NDVI* layer in addition to the four spectral bands was beneficial with a substantial increase of almost 5% in the overall accuracy results and even more with the addition of the *LAI* layer, particularly with SVM. Similar results were found by (10) with an improvement in the classification accuracy when more layers were included in addition to the original spectral bands of the TM image (6 bands plus *NDVI*) instead of using red, near infrared bands and the *NDVI* layer. This result underlines the benefit of using more layers for deriving land cover information.

Results demonstrated that OBIA (NN) performed better than ML. In agreement with this study's results, IKONOS image data sets were analysed for two urban locations by (56) using two approaches, a pixel-based one using ML and an object-based one using fuzzy classification. Significant misclassification errors among the spectrally similar urban land cover types were noticed with the ML classifier, but they were overcome with the object-based classification yielding an increase in accuracy of 11%. Moreover, (40) attest the results of the current study towards using ML and OBIA (NN) focusing on the issue of confusion between spectrally similar classes. They focused on

three indiscernible classes, namely sparse forest, recent cut block, and barren classes. Comparable results were found by (38,43) dealing with the OBIA (NN) and ML classifiers.

The differences between the SVM product and the other classifier products are quite significant due to its capability of locating an optimal separating hyperplane, which concords with (13), who applied SVM for land cover classification of the Gebze district in Turkey using Landsat ETM+ and Terra ASTER images. Results showed that the SVM classifier, especially with the use of the *RBF* kernel, outperforms ML. Similar results were registered with (10) using TM and MODIS remotely sensed data, where SVM outperformed ANN, ML and the Decision Tree. In addition, (19) used DAIS hyperspectral data combined with SVM (*RBF*), ANN, ML and they confirmed the above.

A significant increase of agreement was noticed when increasing the degree of thematic details in the CLC (2006) map by aggregating to level 3 for the SVM classifier. That result disagrees with (59) findings, since the opposite was found when the classification results of an Alpine Monitoring project were compared to the respective land cover maps from the CLC program.

CONCLUSION

The present study was a comparative performance experiment of the popular classifiers ML, ANN, SVM, and OBIA (NN) for LU/LC mapping of a typical Mediterranean fragmented landscape. SVM outperformed the other three classifiers, especially when coupled with the RBF kernel. It dealt with the complex classification scheme with higher success and accuracy than the other non-parametric classifiers, even with a wide number of classes that exceeded the number of classes identified within similar studies (19,22,57). The incorporation of additional dependent layers, together with the four spectral bands of FORMOSAT-2 imagery, as input for the classification algorithms has improved the performance of the SVM (*RBF*) classifier.

Unlike SVM, it seems that ML application achieved a lower mapping accuracy. The other classifiers also showed good performance, proving their strengths in discriminating specific classes. OBIA (NN) has exclusively succeeded in dealing with artificial surfaces with high accuracy compared to the other classifiers and with less accuracy for the agricultural areas, forest and seminatural areas classes. Significant errors were noticed among the spectrally similar artificial surface classes using ML. Moreover, ANN succeeded in classifying agricultural areas and FSNA classes, while ML succeeded in essentially discriminating arable land, sclerophyllous vegetation, and sparsely vegetated areas classes.

To sum up, landscape fragmentation posed a significant challenge to the classifiers and approaches utilized. The results demonstrated the capability of specific classifiers to efficiently extract LU/LC information from the FORMOSAT-2 image. The best performing classifier (SVM) is recommended for operational use under similar frame conditions. Further investigations are anticipated to promote this finding across wider areas.

REFERENCES

1   Giordano F & M Boccone, 2010. Forest fragmentation, urbanization and landscape structure analysis in an area prone to desertification in Sardinia. Present Environment and Sustainable Development, 4:113-128

2   Wu J, 2009. Ecological Dynamics in Fragmented Landscapes. Princeton Guide to Ecology (Princeton University Press) X: 438-444

3   Batistella M, 2000. Extracting earth surface feature information for Land-use/land-cover classifications in Amazonia: the role of remote sensors and processing techniques. In: GIS Brasil 2000, VI Show de Geotecnologias, edited by Anais Fatorgis (Salvador, Brazil) unpaginated CD-ROM

4   Turner W, S Spector, N Gardiner, M Fladeland, E Sterling & M Steininger, 2003. Remote
     sensing for biodiversity science and conservation. Trends in Ecology and Evolution, 18: 306-
     314

5   Nagendra H, D K Munroe & J Southwort, 2004. From pattern to process: Landscape fragmen-
     tation and the analysis of land-use/land-cover change. Agriculture, Ecosystems and Environ-
     ment, 101: 111-115

6   Hall D K, G A Riggs & V V Salomonson, 1995. Development of methods for mapping global
     snow cover using moderate resolution imaging spectroradiometer data. Remote Sensing of
     Environment, 54: 127-140

7   Meiner A, 1996. Evaluations of AVHRR-based land-cover data as input for regional modelling
     of nutrient load to the Baltic Sea. In: HydroGIS 96: Application of Geographic Information Sys-
     tems in Hydrology and Water Resources Management (Proceedings of the Vienna Confer-
     ence, April 1996; IAHS Publication) 689 pp.

8   Foody G M & R A Hill, 1996. Classification of tropical forest classes from Landsat TM data.
     International Journal of Remote Sensing, 17: 2353-2367

9   Hermes L, D Frieauff, J Puzicha, & J M Buhmann, 1999. Support Vector Machines for land
     usage classification in Landsat TM imagery. In: Proceedings of the 1999 IEEE Geoscience
     and Remote Sensing Symposium IGARSS 1999, 348-350

10   Huang C, L S Davis & J R G Townshend, 2002. An assessment of Support Vector Machines
     for land-cover classification. International Journal of Remote Sensing, 23: 725-749

11   Lu D & Q Weng, 2007. A survey of image classification methods and techniques for improving
     classification performance. International Journal of Remote Sensing, 28: 823-870

12   Agarwal R & J K Garg, 2008. Knowledge based classifier of wetlands from coarse resolution
     satellite data. International Journal of Geoinformatics, 4: 17-23

13   Kavzoglu T & I Colkesen, 2009. A kernel functions analysis for Support Vector Machines for
     land-cover classification. International Journal of Applied Earth Observation and Geoinforma-
     tion, 11: 352-359

14   Perumal K & R Bhaskaran, 2010. Supervised classification performance of multispectral im-
     ages. Journal of Computing, 2: 124-129

15   Yu Q, P Gong, N Clinton, G Biging, M Kelly & D Schirokauer, 2006. Object-based detailed
     vegetation classification with airborne high spatial resolution remote sensing imagery. Photo-
     grammetric Engineering & Remote Sensing, 72: 799-811

16   Azimi S M R & S A Zekavat, 2000. Cloud classification using Support Vector Machines. In:
     Proceedings of the 2000 IEEE Geoscience and Remote Sensing Symposium IGARS, 669-671

17   Lennon J J, W E Kunin & S Hartley, 2002. Fractal species distributions do not produce power
     law species area distribution. Oikos, 97: 378-386

18   Pierce N E, M F Braby, A Heath, D J Lohman, J Mathew, D B Rand & M A Travassos, 2002.
     The ecology and evolution of ANT Association in the Lycaenidae (LEPIDOPTERA). Annual
     Review of Entomology, 47: 733-771

19   Pal M & P M Mather, 2003. Support Vector Classifiers for land-cover classification. Map India
     Conference 2003, 11

20   Nemmour H & Y Chibani, 2006. Fuzzy Neural Network architecture for change detection in
     remotely sensed imagery. International Journal of Remote Sensing, 27: 705-717

21   Zhang G P, 2000. Neural Networks for classification: a survey. IEEE Transaction On Systems,
     Man, And Cybernetics, 30: 451-462

22 Kanellopoulos I & G Wilkinson, 1997. Strategies and best practice for Neural Network image classification. International Journal of Remote Sensing, 18: 711-725

23 Leondes C T, 1998. Image Processing and Pattern Recognition, Neural Network Systems Techniques and Application (Academic Press) 372 pp.

24 Paola J D & R A Schowengerdt, 1995. A detailed comparison of Backpropagation Neural Network and Maximum-Likelihood classifiers for urban land use classification. IEEE Transactions on Geoscience and Remote Sensing, 33: 981-996

25 Burges C, 1998. A tutorial on Support Vector Machines for pattern recognition. Data Mining and Knowledge Discovery, 2: 121-167

26 Pal M & P M Mather, 2005. Support Vector Machines for classification in remote sensing. International Journal of Remote Sensing, 26: 1007-1011

27 Tzotsos A & D Argialas, 2008. Support Vector Machine Classification for object-based image analysis. In: Object-Based Image Analysis – Spatial Concepts for Knowledge-Driven Remote Sensing Applications, Section 7 (Springer) 663-677

28 Camps-Valls G, J Gutierrez, G Gomez & J Malo, 2008.On the suitable domain for SVM training in image coding. Journal of Machine Learning Research, 9: 49-66

29 Chi M, R Feng & L Bruzzone, 2008. Classification of hyperspectral remote-sensing data with primal SVM for small-sized training dataset problem. Advances in Space Research, 41: 1793-1799

30 Vapnik V N, 1995. The Nature of Statistical Learning Theory (Springer, New York)

31 Smola A J & B Scholkopf, 2004. A tutorial on Support Vector Regression. Statistics and Computing, 14: 199-222

32 Foody G M & Mathur A, 2004. A relative evaluation of multiclass image classification by Support Vector Machines. IEEE Transactions on Geosciences and Remote Sensing, 42: 1335-1343

33 Blaschke T, S Lang & G J Hay, 2008. Object Based Image Analysis: Spatial Concept for Knowledge Driven RS Applications. Lecture Notes in Geoinformation and Cartography, (Springer) 8536 pp.

34 Giakoumakis M N, I Z Gitas & J San-Miguel, 2002. Object-oriented classification modelling for fuel type mapping in the Mediterranean, using LANDSAT TM and IKONOS imagery - preliminary results. Forest Fire Research & Wildfire Safety, edited by X Viegas, 1-13

35 Flanders D, M H Beyer & J Pereverzoff, 2003. Preliminary Evaluation of eCognition Object-Based Software for Cut Block Delineation and Feature Extraction. International Journal of Remote Sensing, 29: 441-452

36 Thomas A C, P T Strub & P Brickley, 2003. Anomalous satellite-measured Chlorophyll concentrations in the Northern California Current in 2001-2002. Geophysical Research Letters, 30: 8022-8034

37 Laliberte A S, A Rango, K M Havstad, J F Paris, R F Beck, R McNeely & A L Gonzalez, 2004. Object-oriented image analysis for mapping shrub encroachment from 1937 to 2003 in southern New Mexico. Remote Sensing of Environment, 93: 198-210

38 Ivits E, B Koch, T Blaschke, M Jochum & P Adler, 2005. Landscape structure assessment with image grey-values and object-based classification. International Journal of Remote Sensing, 26: 2975-2993

39 Yan P, Y Zhang, D Yang, J Tang, X Yu, H Cheng, S Wang, X Yu, G Liu & X Zhou, 2006. Characteristics of aerosol ionic compositions in summer of 2003 at Lin'An of Yangtze delta region. Acta Meteorologica Sinica, 20: 374-382

40 Brodsky L & L Boravka, 2006. Object-oriented Fuzzy Analysis of remote sensing data for bare soil brightness mapping. Soil & Water Resources,1: 79-84

41 Platt R V & L M Rapoza, 2008. An evaluation of an object-oriented paradigm for land use/land-cover classification. Professional Geographer, 60: 87-100

42 Cleve C, Kelly M, F R Kearns & M Moritz, 2008. Classification of the wild land-urban interface: A comparison of pixel- and object-based classifications using high-resolution aerial photography. Environment and Urban Systems, 32: 317-326

43 Zhou Y & Y Q Wang, 2008. Extraction of impervious surface areas from high spatial resolution imagery by multiple agent segmentation and classification. Photogrammetric Engineering & Remote Sensing, 74: 857–868

44 Soupios P, I Papadopoulos, M Kouli, I Georgaki, F Vallianatos & E Kokkinou, 2007. Investigation of waste disposal areas using electrical methods: a case study from Chania, Crete, Greece. Environmental Geology, 51: 1249–1261

45 Yang M D, T C Su, C H Hsu, K C Chang & A M Wu, 2007. Mapping of the 26 December 2004 Tsunami disaster by using FORMOSAT-2 images. International Journal of Remote Sensing, 28: 3071–3091

46 Pontailler J Y, G J Hymus & B G Drake, 2003. Estimation of Leaf Area Index using ground-based remote sensed NDVI measurements: Validation and comparison with two indirect techniques. International Journal of Remote Sensing, 29: 381-387

47 Knight J F, 2002. Accuracy Assessment of Thematic Maps Using Interclass Spectral Distances. Dissertation, North Carolina State University, USA, 113 pp.

48 Congalton R G, C K Green, 2009. Assessing the Accuracy of Remotely Sensed Data Principles and Practices, 2nd Edition (CRC Press Taylor & Francis Group) 200 pp.

49 Mather P, 2004, Computer Processing of Remotely-Sensed Images: An Introduction, 3rd Edition (John Wiley & Sons Press) 460 pp.

50 Niel V, T G McVicar & T R Datt, 2005. On the Relationship Between Training Sample Size and Data Dimensionality of Broadband Multi-temporal Classification. Remote Sensing of Environment, 98: 468-480

51 ENVI User's Guide, 2009. ENVI On-line Software User's Manual, ITT Visual Information Solutions

52 Cohen J, 1960. A Coefficient of Agreement for Nominal Scales. Educational and Psychological Measurement, 20: 37-46

53 Viera A J, M D Joanne & M Garrett, 2005. Understanding Inter Observer Agreement: The Kappa Statistic. Family Medicine, 37: 360-371

54 Dean A M & G M Smith, 2003. An evaluation of per-parcel land-cover mapping using Maximum Likelihood class probabilities. International Journal of Remote Sensing, 24: 2905-2920

55 Ji M & J R Jensen, 1999. Effectiveness of subpixel analysis in detecting and quantifying urban imperviousness from Landsat Thematic Mapper imagery. Geocarto International, 14: 33-41

56 Liu D and F Xia, 2010. Assessing object-based classification: advantages and limitations. Remote Sensing Letters, 1: 187-194

57 Benz UC, P Hofmann, G Willhauk, I Lingenfelder & M Heyen, 2004. Multiresolution, object-oriented Fuzzy Analysis of remote sensing data for GIS ready information. <u>ISPRS Journal of Photogrammetry & Remote Sensing</u>, 58: 239-258

58 Blaschke T, S Lang & G J Hay, 2008. <u>Object Based Image Analysis: Spatial Concept for Knowledge Driven RS Applications</u>. Lecture Notes in Geoinformation and Cartography (Springer) 817 pp.

59 Steinnocher K, U Schmitt & P Aubrecht, 2000. Potential of automatic classification in Alpine areas for supporting the update of Corine land cover. <u>International Archives of Photogrammetry and Remote Sensing</u>, XXXIII: 207-214